



Exploring new horizons: angiotensin II, angiotensin II type 1 receptor, and renal outer medullary potassium channel interaction in distal convoluted tubule

Kun Zhao¹, Tiantian Han², Linzhen Jia², Libo Wen¹, Renjun Gao³, Xue Li^{1,4}

¹Basic Medical Science College, Qiqihar Medical University, Qiqihar, China

²Pharmacy College, Qiqihar Medical University, Qiqihar, China

³The Sixth Department of Cardiology, The Second Affiliated Hospital of Qiqihar Medical University, Qiqihar, China

⁴Heilongjiang Provincial Key Laboratory of Medicine-food Homologous Resources and Metabolic Disease Prevention and Control, Qiqihar Medical University, Qiqihar, China

Background: This study investigates angiotensin II (Ang II)'s regulatory mechanism on renal outer medullary potassium channel (ROMK) activity in the distal convoluted tubule (DCT) during low potassium intake, focusing on the janus kinase 2 (JAK2) pathway activation mediated by the Ang II type 1 receptor (AT1R).

Methods: Utilizing a low potassium diet mouse model, various methods including patch clamping, reverse transcription-quantitative polymerase chain reaction, Western blotting, and immunohistochemical staining were applied to analyze ROMK channel activity and the expression of related proteins.

Results: The findings reveal that Ang II inhibits ROMK activity in the DCT2 membrane through AT1R activation, with the JAK2 pathway playing a central role. Further, inhibiting JAK2 reverses this effect, indicating its potential in hypertension treatment.

Conclusion: This study provides novel insights into the role of Ang II in renal potassium excretion and hypertension pathophysiology.

Keywords: Angiotensin II, Hypertension mechanisms, Janus kinase 2, Low potassium diet, Renal potassium, ROMK channels

Introduction

Hypertension is one of the most common noncommunicable chronic diseases, which has been identified as a major risk factor for causing deaths, ranking third in global disability-adjusted life years [1]. With the continuous changes in people's way of life, many people are developing high blood pressure, and hypertension in China is increasing yearly [2]. According to a national survey on hypertension

among 451,755 adults, the prevalence of hypertension is 27.9%, and the cure and control rates are 40.7% and 15.3%, respectively [3]. The Heilongjiang province in China belongs to a cold region. The climate is cold, with a large temperature difference between day and night. Moreover, the incidence of hypertension among the northern population is significantly higher than in the south [4].

Hypertension is classified into primary and secondary hypertension, and the pathogenesis of the two types is dif-

Received: January 17, 2024; **Revised:** May 9, 2024; **Accepted:** May 9, 2024

Correspondence: Xue Li

Basic Medical Science College, Qiqihar Medical University, No. 333, Buqiu North Street, Qiqihar, Heilongjiang Province 161006, China.

E-mail: lixue_0720@qmu.edu.cn

ORCID: <https://orcid.org/0009-0002-0710-1907>

© 2025 by The Korean Society of Nephrology

© This is an Open Access article distributed under the terms of the Creative Commons Attribution Non-Commercial and No Derivatives License (<https://creativecommons.org/licenses/by-nc-nd/4.0/>) which permits unrestricted non-commercial use, distribution of the material without any modifications, and reproduction in any medium, provided the original works properly cited.

ferent [5]. About 90% to 95% of cases are primary hypertension, which is caused by nonspecific lifestyle and genetic factors [5]. The remaining 5% to 10% of cases are classified as secondary hypertension, with the main causes being chronic kidney disease, renal artery stenosis, endocrine disorders, etc. [5]. There are many types of Western medicine for treating hypertension with obvious clinical efficacy. Drugs such as spironolactone, nifedipine sustained-release tablets, valsartan, and nitrendipine are widely used [6].

The renal outer medullary potassium channel (ROMK) is an important channel protein that regulates ion homeostasis in the body in the kidneys [7,8]. ROMK mainly facilitates K⁺ crossing of the apical and basolateral membrane cycle, maintains the negative potential of tubular cells, promotes NKCC2 (Na⁺-K⁺-2Cl⁻ cotransporter) and Na⁺-K⁺-ATPase NaCl reabsorption by regulating K⁺ concentration in the tubules, and plays an important role in the urinary concentration mechanism [9]. ROMK is one of the main pathways for renal secretion of K⁺ and is closely related to maintaining body potassium balance [10]. Loss-of-function mutations in the ROMK gene can cause type II Bartter syndrome, characterized by hypokalemia, renal salt wasting, metabolic alkalosis, hypercalciuria, and hypotension, indicating that ROMK is also involved in regulating body water and sodium balance [11].

Angiotensin II (Ang II) acts on the central nervous system, increasing the production of antidiuretic hormones and affecting the smooth muscles of veins and arteries, causing vasoconstriction [12]. The renin-angiotensin system consists of multiple enzymes, peptides, and receptors, and plays an important role in the occurrence, development, and treatment of cardiovascular diseases such as hypertension, coronary atherosclerotic heart disease, and heart failure [13]. Ang II is the key effector peptide of this system, which regulates blood pressure by stimulating aldosterone secretion via Ang II type 1 receptor (AT1R) and conducting water and sodium regulation [14].

AT1R can lead to the constriction of small arterial vessels, increase systemic vascular resistance, and result in elevated blood pressure. Ang II also induces aldosterone synthesis and secretion by stimulating renal glomerular AT1R, resulting in sodium and water retention [15]. The renin-angiotensin-aldosterone system plays a cascading role of a proteolytic enzyme, continuously hydrolyzing circulating precursor hormones to produce Ang II, which then acts

by activating G protein-coupled type 1 Ang II receptors and mediating its effects [15].

Janus kinase 2 (JAK2) is closely related to hypertension, and there have been multiple studies reporting its correlation. After blocking JAK2, it is possible to protect mice against hypoxia-induced pulmonary arterial hypertension by suppressing pulmonary arterial smooth muscle cell proliferation [16]. JAK2 is involved in pulmonary arterial remodeling, and studies have found that JAK2 may be one of the potential therapeutic targets for idiopathic pulmonary fibrosis associated with pulmonary arterial hypertension [17]. Additionally, studies report that using JAK2 inhibitors to suppress the JAK2 signaling pathway can treat erythrocytosis-associated pulmonary arterial hypertension [18].

This study investigates the regulation of the JAK2 signaling pathway by Ang II in a low potassium diet, which inhibits renal K⁺ excretion. It is initially believed that Ang II binds with AT1R and upregulates JAK2, activating the JAK2 signaling pathway, suppressing the activity of ROMK channels in the distal renal tubules, inhibiting renal K⁺ excretion, and improving hypertension. It also makes factors such as Ang II, AT1R, and JAK2 target hypertension treatment, providing a new theoretical basis for treating hypertension.

Methods

Animal model construction

In the animal experiments, 100 C57BL/6 mice that had just been weaned (3–5 weeks old) were selected, irrespective of sex. Their feeding was standardized, and food and water intake were not restricted. These 100 mice were randomly divided into 10 groups, with 10 mice in each group. Under the condition of free access to water, regular potassium diet (1.0% w/w potassium content) was provided to 20 mice, and low potassium diet (<0.05% w/w potassium content) was provided to 80 mice for 7 days. The normal potassium (NK) group consists of 10 mice on a normal potassium diet, while the low potassium (LK) group consists of 80 mice on a low potassium diet. The feed we use is purchased from SSNIFF Spezialdiäten GmbH (Soest). We used 10 normal potassium diet-fed mice and 40 low potassium and low oxygen diet-fed mice to prepare the distal convoluted tubules (DCT). An additional 40 LK-induced mice were randomly

divided into four groups (n = 10), including the control group (LK-induced mice), the Ang II group (LK-induced mice treated with Ang II), the Ang II + losartan group (LK-induced mice treated with Ang II and losartan), and the Ang II + AG490 group (LK-induced mice treated with Ang II and AG490). After LK induction, we used an Alzet osmotic minipump (Alza Corp.) to subcutaneously inject Ang II (1.5 mg/kg/day, A9847; Sigma Chemical) into the neck of the mice once a day. The control group mice were subcutaneously injected with 0.9% physiological saline [19]. We added losartan (10 mg/kg/day, SML3317; Sigma Chemical) or its solvent control (ethanol diluted 4:1,000) to the drinking water of mice [20]. JAK2 inhibitor AG490 (10 mg/kg/day, T3434; Sigma Chemical) was administered by intraperitoneal injection once daily. The control group mice were injected intraperitoneally with saline solution [19]. On the eighth day since the start of the experiment, we placed each group of mice in a metabolic cage to collect urine for 24 hours. After the experiment, we euthanized the mice. The Animal Experiment Center of Qiqihar Medical College provided the experimental animals.

The experimental animal protocol has been approved by the Qiqihar Medical College Animal Ethics Committee (No. QMU-AECC-2021-77, No. QMU-AECC-2022-90, No. QMU-AECC-2023-104).

Preparation of the distal convoluted tubule of the kidney

The NK and LK mouse models were constructed using the methods described earlier. After euthanizing the mice with spinal cord transection, their abdominal cavities were opened to expose the kidneys. The left kidney was perfused with L-15 nutrient solution (11415064; Gibco) containing 2 mL of type II collagenase (C2-BIOC; Sigma Chemical). The perfused kidney was then dissected, and the medulla was removed. The cortex was cut into small pieces approximately 1 mm² in size and incubated at 37 °C in a water bath for 50 minutes. After three washes with nutrient solution, the DCT2, representing the DCT of the kidney, was isolated under a stereomicroscope. The isolated DCT2 segments were placed on coverslips coated with poly-L-lysine and transferred to an inverted microscope. Using a microelectrode, the DCT2 segments were incised to expose the tubular lumen for sealing.

The mouse DCT2 segments were divided into groups as follows: NK + control group, comprising mice fed a normal

potassium diet with isolated DCT2 segments left untreated; NK + Ang II group, with DCT2 segments from NK-fed mice treated with 1, 10, and 100 nM Ang II (A9847); LK + control group, where DCT2 segments from LK-fed mice remained untreated; LK + Ang II group, with DCT2 segments from LK-fed mice treated with 1, 10, and 100 nM Ang II; LK + losartan + Ang II group, where DCT2 segments from LK-fed mice were treated with 100 nM Ang II and 20 μM losartan; LK + PD123319 + Ang II group, where DCT2 segments from LK-fed mice were treated with 100 nM Ang II and 10 μM PD123319; LK + AG490 group, with DCT2 segments from LK-fed mice treated with 1 μM AG490; LK + AG490 + Ang II group, where DCT2 segments from LK-fed mice were treated with 100 nM Ang II and 1 μM AG490 [21].

Single-channel patch clamp technique

Cell-level investigations on various mice using the single-channel patch clamp technique were involved. Experiments were conducted using cell-attached and single-channel patch clamp recording modes to test different samples. The current recordings of individual K⁺ channels were performed using Axon200B amplifier (Axon), with a low-pass filter frequency of 1 kHz. The recorded data is digitized through an Axon interface (Digidata 1332; Molecular Devices) with a sampling rate of 4 kHz. For single-channel recording, the pipette solution contained 140 nM KCl, 2 nM MgCl₂, 1 nM EGTA, and 10 nM HEPES (pH 7.4 adjusted with KOH), while the bath solution contained 135 nM NaCl, 5 nM KCl, 2 nM MgCl₂, 1.8 nM CaCl₂, 5 nM glucose, and 10 nM HEPES (pH 7.4 adjusted with NaOH).

To calculate the probability of channel opening (Po), we selected a channel recording with a current level stable for at least 5 minutes and a duration of less than 3 ms to determine the baseline of the closed state. The channel Po is calculated by multiplying the number of channels (N) and the probability of openness (NPo). The NPo is calculated from a data sample of 60 seconds at a steady state using the following formula: $NPo = \sum (1t_1 + 2t_2 + \dots + it_i)$, where it represents the time that the channel is open at each level [22].

Recording and analysis of whole-cell patch clamp (20927043)

In the examination of the DCT2 tubular membrane in

various mice, whole-cell patch clamp recordings were performed using an Axon 200B amplifier to measure the reversal potential of K⁺ current and the tertiapin-Q (TPNQ)-sensitive K⁺ current. The pipette tip was filled with a solution containing 140 mM KCl, 2 mM MgATP, 1 mM EGTA, and 10 mM HEPES, and was loaded with amphotericin B (20 µg/0.1 mL, A9528; Sigma Chemical). The bath solution consisted of 140 mM KCl, 2 mM MgCl₂, 1.8 mM CaCl₂, and 10 mM HEPES (pH 7.4). Once a high-resistance seal (>2 GΩ) was achieved, membrane capacitance was monitored until whole-cell configuration was established. Currents were low-pass filtered at 1 kHz and digitized through the Axon interface (Digidata 1332) at a sampling rate of 4 kHz [22]. Data analysis was conducted using the pClamp 9.0 software system (Axon).

Western blot

The renal cortex tissue was lysed using radio-immunoprecipitation assay lysis buffer (P0013B; Beyotime Biotechnology) to extract total protein. The protein concentration of the renal cortex protein solution obtained was determined using a BCA assay kit (P0010S; Beyotime Biotechnology). Each protein sample was loaded for electrophoresis once on a sodium dodecyl sulfate gel and then transferred to a nitrocellulose (NC) membrane. Following membrane transfer, the NC membrane was blocked with 5% skim milk, washed, and subsequently incubated overnight with the following antibodies: ROMK polyclonal antibody (1:1,000, ABP55003; Amyjet Scientific), rabbit anti-AT1R (1:1,000, #ab124505; Abcam), rabbit anti-AT2R (1:1,000, #ab92445; Abcam), rabbit anti-JAK2 (1:1,000, #ab108596; Abcam), rabbit anti-pJAK2 (1:1,000, #ab32101; Abcam), rabbit anti-β-actin (1:1,000, #ab8227; Abcam). After incubation at 4 °C and washing with phosphate-buffered saline (PBS) with Tween 20 (PBST), the rabbit immunoglobulin G (IgG) secondary antibody labeled with horseradish peroxidase (1:1,000, sc-2357; Santa Cruz) was incubated for 1 hour at room temperature. Then clean it with PBST three times, each time for 5 minutes. After cleaning, visualize using ECL reagent (32109; Thermo Fisher) on the imaging apparatus. Use ImageJ software for quantitative analysis of strip grayscale values. The gray value of the target protein strip is calibrated by dividing it by the gray value of the internal reference β-actin strip, thereby obtaining the relative con-

tent of the target protein in the sample. The protein blot images were analyzed using ImageJ2x software [23,24]. At least three biological replicates were performed for each experimental group.

Immunofluorescence staining

Renal cortex tissue was embedded in paraffin, sectioned into 5 µm thick slices, and subjected to routine deparaffinization (three times with xylene, 5 minutes each) and hydration (thrice with 100% ethanol, once with 90%, 80%, 70% ethanol, and PBS each, for 5 minutes per step). Subsequently, antigen retrieval was performed using citrate buffer, followed by incubation in 1% bovine serum albumin (BSA) blocking solution at room temperature for 1 hour. The sections were then incubated overnight at 4 °C with primary antibodies: ROMK antibody (GTX54775, anti-rat, 1:100; GeneTex) and MUC1 antibody (#ab4538, anti-mouse, 1:100; Abcam). After washing with PBS, the sections were incubated at room temperature for 2 hours with IgG-Alexa Fluor 488 antibody (A-11006, anti-rat, 1:100; Invitrogen) and IgG-Alexa Fluor 568 antibody (A-11004, anti-mouse, 1:100; Invitrogen). Following DAPI staining, the sections were observed using a laser confocal microscope (SP5; Leica) [25].

Measurement of urinary potassium, blood potassium, and sodium levels

Mice were randomly divided into NK and LK groups, with 10 mice in each group, and placed in metabolic cages for 24 hours to record weight and urine output. Urinary potassium ion concentrations were measured using the potassium ion test kit (C001-2-1) from Nanjing Jiancheng Bioengineering Research Institute. The results were quantified in nmol/min per 100 g body weight [26]. Blood potassium and sodium ion concentrations were determined using flame photometry (FP8800; KRUS) [27].

RNA extraction and sequencing

Renal cortex tissues from hypertensive model mice were collected for this study. Three samples were obtained per group, and total RNA was extracted using TRIzol reagent (15596026; Invitrogen). The concentration and purity of RNA samples were assessed using a Nanodrop 2000 spec-

trophotometer (1,011 U; Thermo Fisher Scientific). Samples with an RNA integrity number of ≥ 7.0 and a 28S:18S ratio of ≥ 1.5 were selected for subsequent experiments.

CapitalBio Technology in Beijing prepared and sequenced our sequencing library. The RNA amount for each sample is 5 μ g. We used the Ribo-Zero Magnetic Kit (MRZE706; Epicentre Technologies) to remove ribosomal RNA from total RNA. The NEB Next Ultra RNA Library Prep Kit (#E7775; New England Biolabs) was used to prepare the libraries required for Illumina sequencing. Then, use NEB Next First Strand Synthesis Reaction Buffer (5 \times) to cut the RNA segment into fragments with a length of about 300 base pairs. The first strand of complementary DNA (cDNA) is synthesized using reverse transcriptase primers and random primers, while the second strand of cDNA is synthesized in the reaction buffer of dUTP Mix (10 \times) for the second strand synthesis. We performed 3' end repair of cDNA fragments and added poly(A) tail and sequencing adapters for ligation. Next, we ligate Illumina sequencing adapters and use the USER enzyme (#M5508; New England Biolabs) to degrade the second strand of cDNA to establish a strand-specific library. Then, we amplified the library DNA and enriched it with polymerase chain reaction (PCR). Finally, we assessed the quality of the library using Agilent 2100 and quantified the library using KAPA Library Quantification Kit (KK4844; KAPA Biosystems). Finally, we loaded the library onto the NextSeq CN500 (Illumina) for paired-end sequencing [26,28].

Quality control of sequencing data and alignment to the reference genome

The quality of paired-end reads in the raw sequencing data was assessed using FastQC software version 0.11.8 (Babraham Bioinformatics). Preprocessing of the raw data was conducted with Cutadapt software version 1.18, which involved the removal of Illumina sequencing adapters and poly(A) tail sequences. Subsequently, a Perl script was executed to eliminate reads with N content exceeding 5%. The FASTX Toolkit software version 0.0.13 was utilized to extract reads with at least 20 bases and a quality score above the specified threshold, accounting for 70% of the data. Following this, BMap software was employed for the repair of paired-end sequences. Finally, the filtered high-quality read fragments were aligned to the mouse reference genome using hisat2 software (version 0.7.12) [29].

Bioinformatics analysis

The messenger RNA (mRNA) read count data were subjected to differential expression analysis using the “edgeR” package in the R language, with criteria set at $|\log_2FC| > 1$ and p-value of < 0.05 . For protein interaction analysis between genes, the STRING database (<https://string-db.org/>) was utilized, and visualization of the protein-protein interaction network required the use of Cytoscape software version 3.5.1 (<https://cytoscape.org/>). Statistical significance was considered for p-values of < 0.05 using the “ClusterProfiler” package in R (R Foundation for Statistical Computing), for conducting Kyoto Encyclopedia of Genes and Genomes (KEGG) pathway enrichment analysis of differentially expressed genes [30,31].

Reverse transcription-quantitative polymerase chain reaction

Total RNA was extracted from tissues and cells using TRIzol reagent, and the purity and concentration of total RNA were determined using the nanodrop2000 ultraviolet spectrophotometer (nanodrop). Perform RNA reverse transcription to generate cDNA according to the instructions of TaqMan MicroRNA Assays Reverse Transcription primer (Applied Biosystems) or PrimeScript RT reagent Kit (Takara), and design primers for mouse AT1R and AT2R, which were synthesized by Takara (Supplementary Table 1, available online). By using TaqMan Multiplex real-time fluorescence quantitative PCR detection and ABI7500 quantitative PCR instrument (Applied Biosystems) with reaction conditions set as 95 °C pre-denaturation for 10 minutes, 95 °C denaturation for 10 seconds, 60 °C annealing for 20 seconds, 72 °C extension for 34 seconds, repeated for a total of 40 cycles. Temperature was increased from 65 to 95 °C for the melting curve analysis of PCR products. Using glyceraldehyde 3-phosphate dehydrogenase as the internal reference primer, the relative transcription level of the target gene was calculated by the $2^{-\Delta\Delta Ct}$ method [32]. $\Delta Ct = Ct(\text{target gene}) - Ct(\text{reference gene})$, $\Delta\Delta Ct = \Delta Ct(\text{experimental group}) - \Delta Ct(\text{control group})$, the relative transcription level of target gene mRNA = $2^{-\Delta\Delta Ct}$. Repeat each experiment at least three times.

Immunohistochemical staining

The renal cortex tissue was embedded in paraffin and then cut into 5 μm -thick slices. Then perform the routine dewaxing treatment (three times with xylene, 5 minutes each) and hydration treatment (three times with 100% alcohol, one time each with 90%, 80%, 70% alcohol, and PBS, 5 minutes each time). Subsequently, antigen microwave heat retrieval was performed using citrate buffer. After that, the slides were blocked with 1% BSA blocking solution at room temperature for 1 hour. Then, primary antibodies (anti-rabbit anti-AT1R: 1:500, #ab124505, Abcam; anti-rabbit anti-JAK2: 1:100, #ab108596, Abcam) were incubated overnight at 4 °C. After PBS washing, IgG labeled with HRP (BA1054; Boster Bio) was incubated at room temperature for 1 hour, followed by DAB reagent (AR1000; Boster Bio) staining and terminated with tap water. Finally, the samples were stained with hematoxylin-eosin and examined under a microscope after dehydration with an alcohol gradient and mounting on a slide [33,34]. Image acquisition was performed using a microscope (DM2500; Leica). Six consecutive non-repetitive fields of renal cortex tissue slices were extracted for each mouse, and the staining intensity was evaluated using IHC Profiler in ImageJ software (Media Cybernetics Inc.).

Statistical analysis

This study employed IBM SPSS version 21.0 (IBM Corp.) for data statistical analysis. The measurement data is represented by the mean value plus the standard deviation. The non-paired t test is used to compare two sets of data. One-way analysis of variance (ANOVA) compares multiple data sets, and the Tukey test is used for *post-hoc* analysis. Repeated measures ANOVA was used to compare the data of different groups at different time points, and the Bonferroni method was used for *post-hoc* analysis. The difference is considered statistically significant when the p-value is less than 0.05.

Results

Ang II can inhibit the activity of ROMK channels in the DCT2 tubular membrane in a low potassium diet

To investigate the effect of Ang II on the activity of ROMK channels in the DCT2 tubular membrane, we extracted the renal DCT tubular membranes of C57BL/6 mice fed with normal and low potassium diets. We tested the activity of ROMK channels in each group using single-channel and whole-cell patch clamp experiments. Using the single-channel patch clamp technique, the NPo detection results of the ROMK channel showed that at the clamping voltage of 0 mV, Ang II significantly suppressed the activity of the ROMK channel in the luminal membrane of DCT2 in a dose-dependent manner in the low potassium diet group. In the separated DCT2 tubular membranes of mice on a normal potassium diet, no consistent effect was observed, and only a slight decrease in ROMK channel activity was demonstrated with 100 nM Ang II, indicating that Ang II can significantly inhibit ROMK channel activity (Fig. 1A). According to the literature, Ang II inhibits the ROMK channel activity in a dose-dependent manner in LK rather than NK rats. This effect is due to potassium depletion which upregulates the expression of Src family protein tyrosine kinases (PTKs), including cSrc. The phosphorylation of the ROMK channel by cSrc enhances its endocytosis, reducing potassium secretion and leading to elevated blood pressure [20,35]. TPNQ-sensitive whole-cell potassium currents were recorded at a clamping voltage of -60 mV using the whole-cell patch clamp recording mode. In the normal potassium diet, only 100 nM Ang II showed inhibition of potassium current intensity sensitive to TPNQ in the DCT2 tubular membrane, while in the low potassium diet, Ang II significantly inhibited the potassium current intensity sensitive to TPNQ in DCT2 tubular membrane in a dose-dependent manner (Fig. 1B, C).

Western blot analysis showed that in a normal diet, only 100 nM Ang II tended to decrease the expression of ROMK channel protein in the DCT2 tubular membrane. However, in a low potassium diet, Ang II significantly inhibited the expression of ROMK channel protein in the DCT2 tubular membrane in a dose-dependent manner (Fig. 1D, E). In addition, compared to a normal potassium diet, the urinary potassium excretion in mouse kidneys on a low potassium

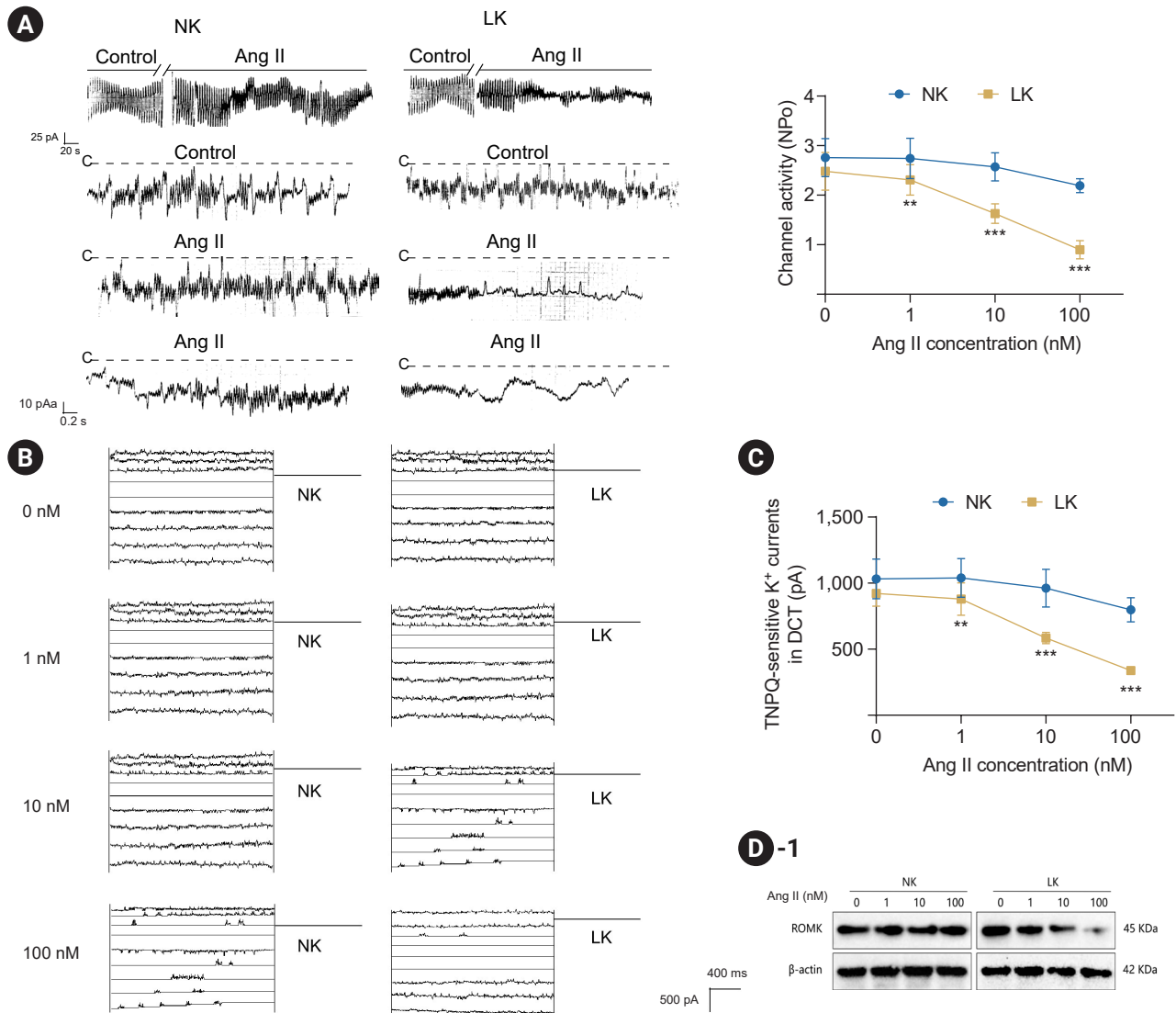


Figure 1. Effect of Ang II on ROMK channel activity and protein expression in the lumen membrane of DCT2 in a low potassium diet. (A) Single-channel patch clamp technique was used to detect the ROMK channel activity in the lumen membrane of DCT2 in each group. The representative traces of ROMK channel activity induced by 100 nM Ang II in normal and low potassium diets are shown in the left and middle panels. The closed state of the channel ("C") is represented by a dashed line. The current ROMK channel activity is indicated by the short bar on the right side of each trace. The dose-response curve of Ang II on ROMK channel activity in the lumen membrane of DCT2 induced by normal and low potassium diets is shown in the right panel. (B) Whole-cell patch clamp technique was used to measure the tertiapin-Q (TPNQ)-sensitive K⁺ current and voltage stimulation protocol in the lumen membrane of DCT2 in each group. (C) Statistical analysis of the TPNQ-sensitive K⁺ current in the lumen membrane of DCT2 in each group measured by the whole-cell patch clamp technique. (D) Western blot analysis of ROMK protein expression in the lumen membrane of DCT2 in each group. (E) Immunofluorescence detection of ROMK protein expression in various DCT2 tubular membranes. (F) Measurement of urinary potassium excretion in different groups of mice. (G) Assessment of urine volume in various mice. (H) Evaluation of blood potassium ion levels in various mice. (I) Analysis of sodium ion levels in various mice.

Ang II, angiotensin II; BW, body weight; DCT, distal convoluted tubule; LK, low potassium; NK, normal potassium; NPo, number of channels × probability of openness; ROMK, renal outer medullary potassium channel.

p* < 0.01 and *p* < 0.001, significantly different between the two groups; *n* = 10.

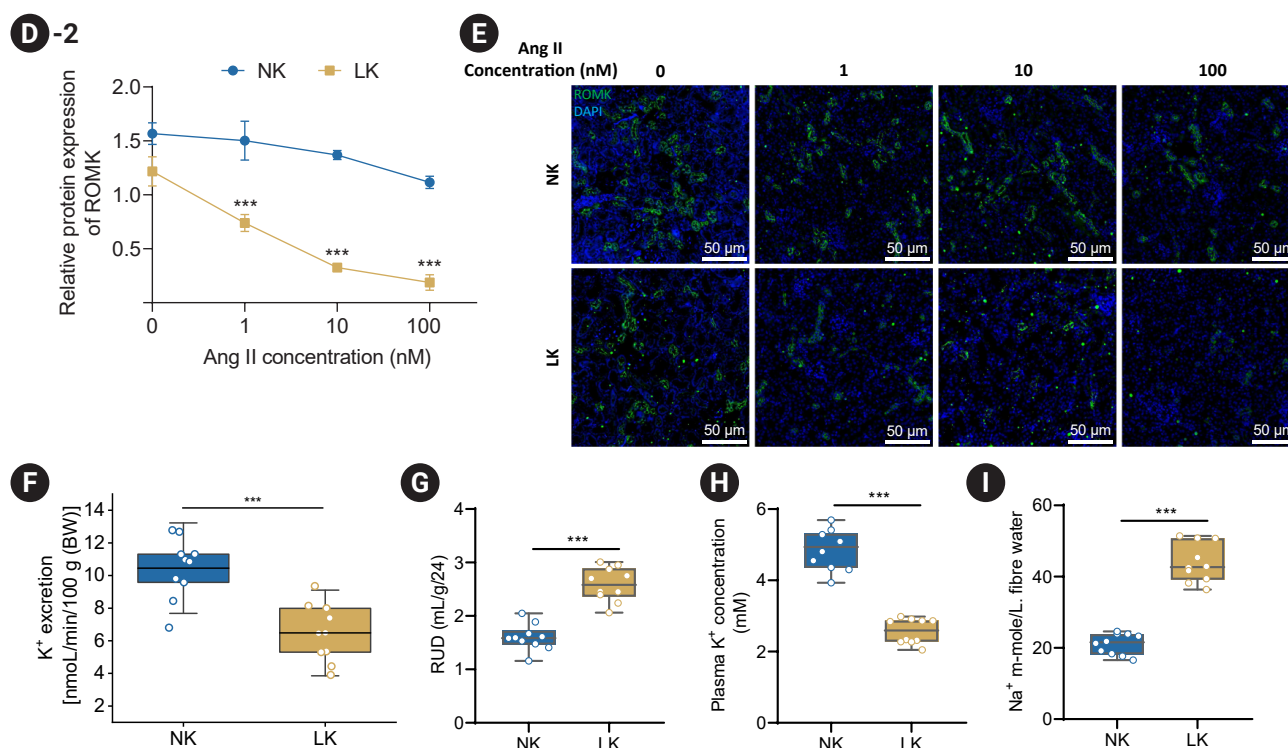


Figure 1. (Continued).

diet was significantly reduced (Fig. 1F). Compared to mice on a normal diet, those on a low potassium diet showed a significant increase in urine volume (Fig. 1G). Additionally, mice on a low potassium diet exhibited significantly reduced potassium ion levels in their blood and increased sodium ion levels compared to those on a normal potassium diet (Fig. 1H, I).

The above results indicate that Ang II in a low potassium diet could inhibit the activity of the ROMK channel in the DCT2 lumen membrane.

Ang II inhibits the activity of the ROMK channel in the tubular membrane of DCT2 by activating the AT1R receptor

To determine whether AT1R or AT2R mediates the inhibitory effect of Ang II on ROMK channels, we first pretreated the DCT2 of LK mice with AT1R antagonist losartan (20 μM) and then exposed them to Ang II. It turned out that losartan eliminated the inhibitory effect of Ang II on the activity of ROMK channels and TPNQ-sensitive potassium currents (Fig. 2A, C). In DCT2 pretreated with AT2R antag-

onist PD123319 (10 μM), the inhibitory effects of Ang II on the activity of ROMK channels and TPNQ-sensitive potassium currents were the same as those in DCT2 without any receptor antagonist treatment (Fig. 2B, D). Next, we detected the expression of ROMK, AT1R, and AT2R and found that compared with the LK+ control group, the ROMK protein expression in the DCT2 tubular membrane of the LK+ Ang II group was significantly decreased, while the expression of AT1R and AT2R was significantly increased. In the LK+ losartan+ Ang II group, the expression of ROMK channel protein in the membrane of the DCT2 lumen was significantly increased, and the expression of AT1R was significantly decreased. In the LK+ losartan+ PD123319 group, the expression of ROMK channel protein in the membrane of the DCT2 lumen was unchanged, and the expression of AT2R was significantly decreased (Fig. 2E-H). Therefore, the above results indicate that AT1R receptors may mediate the inhibitory effect of Ang II on the ROMK channel of the DCT2 tubular membrane.

We orally administered losartan (10 mg/kg/day) to the mice fed by LK for 8 days. We performed immunohisto-

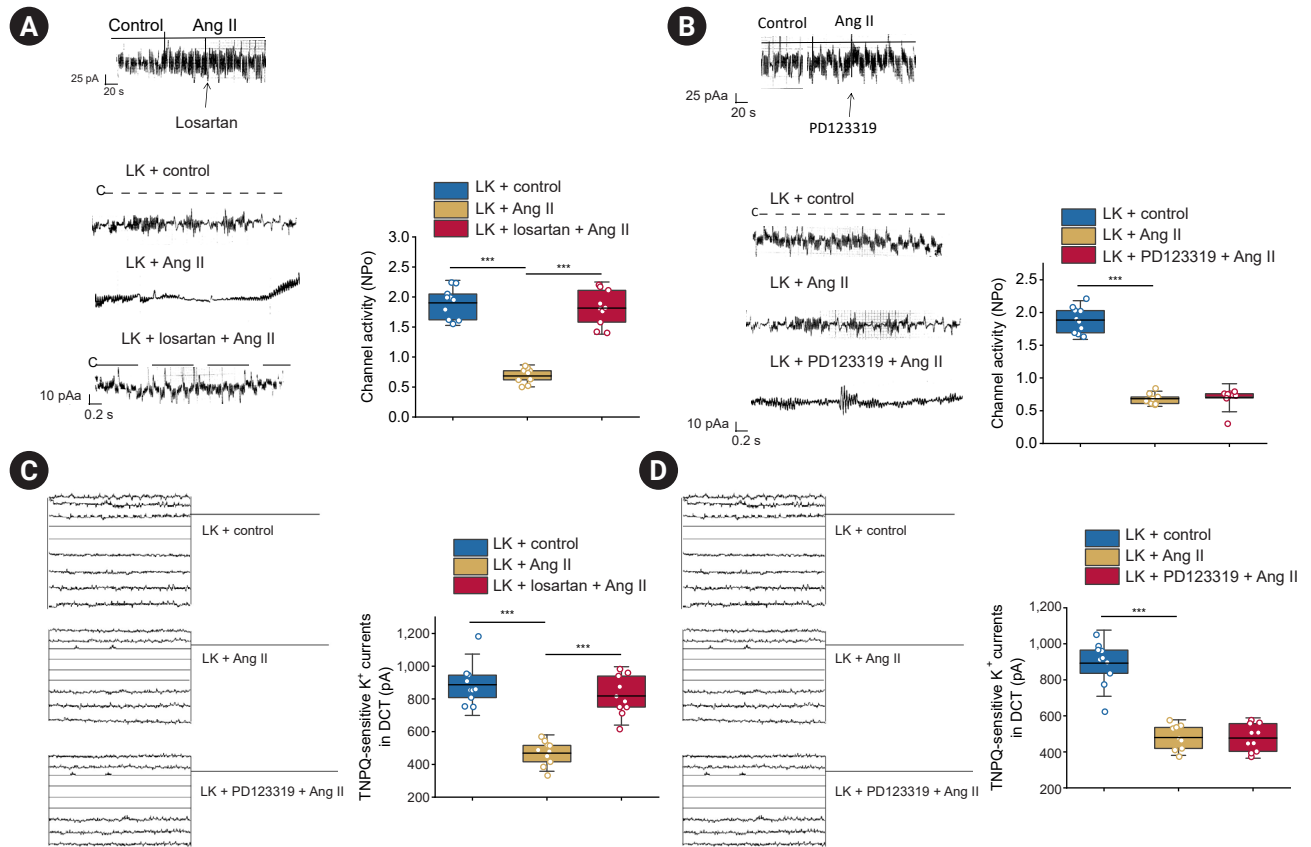


Figure 2. Ang II-mediated regulation of ROMK channel activity in the lumen membrane of DCT2 via AT1R receptor. (A) Single-channel patch clamp technique was used to examine the effect of AT1R antagonist losartan in combination with Ang II on ROMK channel activity in the lumen membrane of DCT2. The closed state of the channel ("C") is represented by a dashed line. The current ROMK channel activity is indicated by the short bar on the right side of each trace. (B) Single-channel patch clamp technique was used to examine the effect of AT2R antagonist PD123319 in combination with Ang II on ROMK channel activity in the lumen membrane of DCT2. 1–3 indicate ROMK channel activity measured at different time points. The closed state of the channel ("C") is represented by a dashed line. The current ROMK channel activity is indicated by the short bar on the right side of each trace. (C) Measurement of the strength of tertiapin-Q (TPNQ)-sensitive K⁺ current in the lumen membrane of DCT2 in each group treated with AT1R antagonist losartan in combination with Ang II, with the left panel showing the current changes and the right panel showing the statistical analysis. (D) Measurement of the strength of TPNQ-sensitive K⁺ current in the lumen membrane of DCT2 in each group treated with AT2R antagonist PD123319 in combination with Ang II, with the left panel showing the current changes and the right panel showing the statistical analysis. (E) Effect of AT1R antagonist losartan in combination with Ang II on ROMK and AT1R protein expression in the lumen membrane of DCT2 as detected by Western blotting. (F) Effect of AT1R antagonist losartan in combination with Ang II on AT1R gene expression in the lumen membrane of DCT2 as detected by reverse transcription polymerase chain reaction (RT-PCR). (G) Effect of AT2R antagonist PD123319 in combination with Ang II on ROMK and AT2R protein expression in the lumen membrane of DCT2 as detected by Western blotting. (H) Effect of AT2R antagonist PD123319 in combination with Ang II on AT2R gene expression in the lumen membrane of DCT2 as detected by RT-PCR. (I) Immunohistochemical detection of AT1R protein expression in the renal cortex tissue of each group of mice. (J) Western blot analysis of ROMK and AT1R protein expression in the renal cortex tissue of each group of mice. (K) Single-channel patch clamp technique was used to examine the effect of losartan in combination with Ang II on ROMK channel activity in the lumen membrane of DCT2 in LK-induced mice, with 1–3 indicating ROMK channel activity measured at different time points. The closed state of the channel ("C") is represented by a dashed line. The current ROMK channel activity is indicated by the short bar on the right side of each trace. (L) Measurement of the strength of TPNQ-sensitive K⁺ current in the lumen membrane of DCT2 in LK-induced mice treated with losartan in combination with Ang II, with the left panel showing the current changes and the right panel showing the statistical analysis. (M) Measurement of urinary potassium excretion in each group of mice.

Ang II, angiotensin II; AT1R, Ang II type 1 receptor; BW, body weight; DCT, distal convoluted tubule; LK, low potassium; NK, normal potassium; NPo, number of channels × probability of openness; ROMK, renal outer medullary potassium channel.

****p* < 0.001, significantly different between the two groups; *n* = 10.

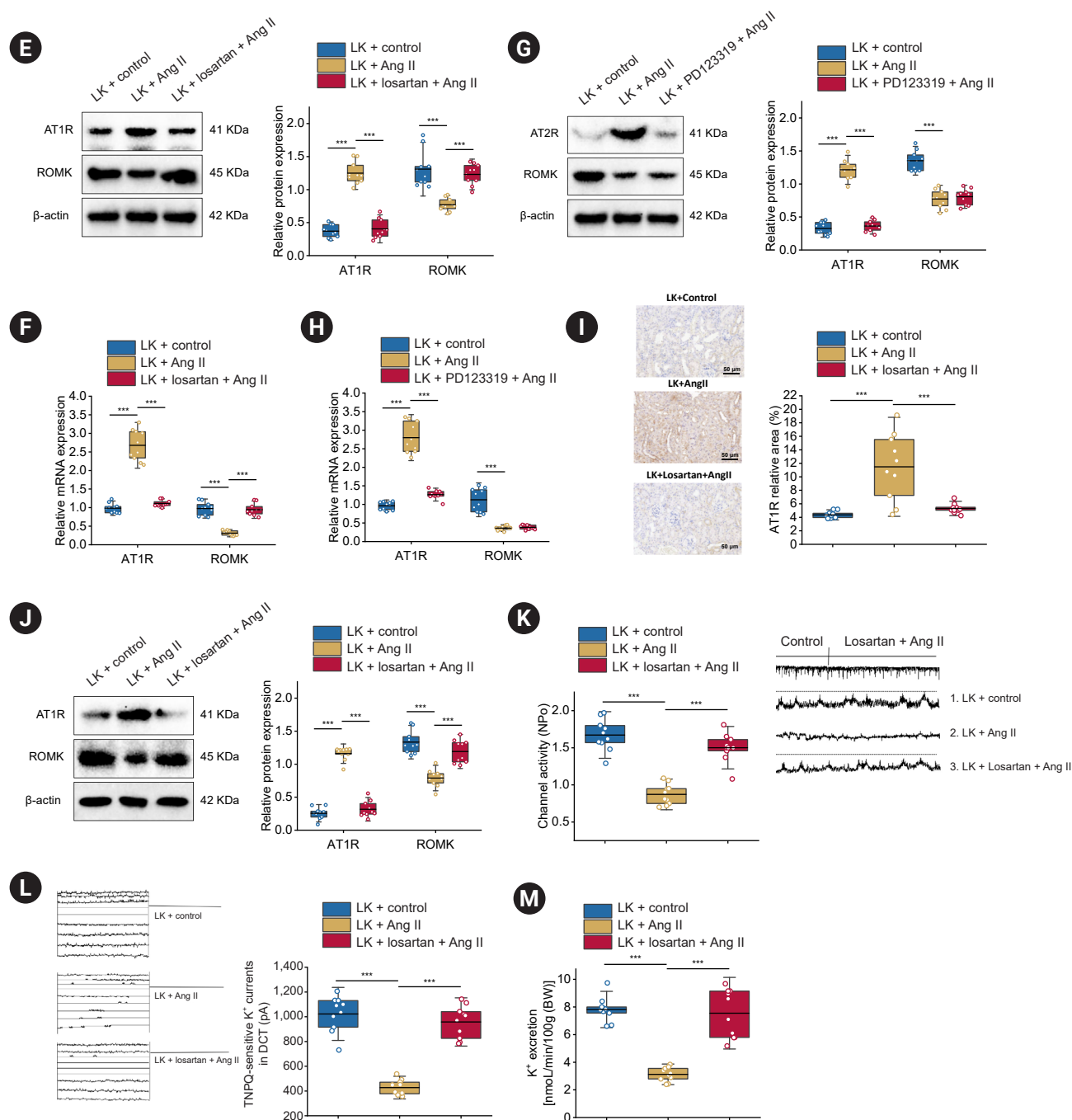


Figure 2. (Continued).

chemistry and Western blot to detect the expression of ROMK and AT1R proteins in mouse renal cortex tissue. It was found that compared with the LK group, the expression of ROMK protein was significantly reduced, and AT1R protein expression was significantly increased in the renal cortex tissue of mice in the LK + Ang II group. In the liter-

ature [36,37], Ang II stimulation induces the expression of BACH1, allowing its translocation into the nucleus, where it facilitates binding to the AT1R promoter region, leading to an upregulation of AT1R expression and thereby enhancing the Ang II-AT1R interaction. In the LK + Ang II + losartan group, the expression of ROMK protein in mouse

renal cortex tissue was significantly increased, and the expression of AT1R protein was significantly decreased (Fig. 2I, J). Meanwhile, we also examined the ROMK channel activity and TPNQ-sensitive potassium current intensity in the DCT2 apical membrane of each group of mice. The results showed that compared with the LK group, the ROMK channel activity and TPNQ-sensitive potassium current intensity in the DCT2 luminal membrane of mice in the LK + Ang II group were significantly inhibited. In the LK + Ang II + losartan group, the activity of ROMK channels and the intensity of TPNQ-sensitive potassium currents in the DCT2 luminal membrane were significantly increased (Fig. 2K, L). In addition, compared with the LK group, the urinary potassium excretion in the kidneys of mice in the LK + Ang II group was significantly reduced, while in the LK + Ang II + losartan group, the urinary potassium excretion in the kidneys of mice was significantly increased (Fig. 2M).

Based on the above results, we conclude that Ang II may inhibit the activity of DCT2 luminal ROMK channels by activating AT1R receptors.

Transcriptome sequencing screening of key pathways in Ang II-induced hypertension

A 21-day hypertension mouse model was constructed by burying a pump that releases Ang II slowly *in vitro*. Transcriptome sequencing analysis was performed on the mouse renal cortex, followed by data quality control and mRNA identification. Differential analysis was performed using the “edgeR” package in R language based on the identified mRNA count, and the results revealed 341 upregulated genes and 181 downregulated genes (Fig. 3A). Next, we performed Gene Ontology and KEGG enrichment analysis for the differentially expressed genes (Fig. 3B, C), and the results showed that these genes were mainly involved in biological processes such as synapse organization and regulation of membrane potential.

Signaling pathways include cyclic adenosine monophosphate signaling, JAK-signal transducer and activator of transcription (STAT) signaling, and insulin signaling pathways. Meanwhile, literature reports suggest a close association between JAK-STAT signaling pathways and vascular diseases, in which JAK2 is involved in various processes related to pulmonary artery remodelings, such as smooth muscle cell proliferation, endothelial dysfunction, and in-

flammation, and it can promote vascular activation. Therefore, we continued to explore the regulatory roles of a low potassium diet and Ang II on the DCT2 tubular membrane JAK2 signaling pathway. We investigated the effect of Ang II on the expression of JAK2 signaling pathway proteins in the DCT2 tubular membrane through Western blot analysis under a low potassium diet. The results showed that under normal dietary conditions, only 100 nM of Ang II can promote the phosphorylation of the JAK2 protein of the ROMK channel in the tubular membrane of the DCT2. However, under a low potassium diet, the promoting effect of Ang II showed dose dependency and significantly promoted the phosphorylation of JAK2 protein in the DCT2 tubular membrane (Fig. 3D).

Therefore, we can conclude that under a low potassium diet, Ang II can promote the activation of the JAK2 signaling pathway in the luminal membrane of DCT2.

Inhibiting the JAK2 signaling pathway can activate the activity of the DCT2 luminal ROMK channel

To further investigate the effect of the JAK2 signaling pathway on the activity of the ROMK channel in the apical membrane of the DCT2, we pretreated DCT2 extracted from LK mice with JAK2 inhibitor AG490 (1 μ M) and detected ROMK channel activity and TPNQ-sensitive whole-cell potassium current through single-channel patch clamp and whole-cell patch clamp experiments. Results showed that compared with the LK group, the DCT2 luminal ROMK channel activity, and TPNQ-sensitive whole-cell potassium current were significantly increased in the LK + AG490 group (Fig. 4A, B). Meanwhile, after performing Western blot detection of ROMK and JAK2 signaling proteins, we found that compared to the LK group, the LK + AG490 group exhibited a significant increase in ROMK protein expression and a significant decrease in phosphorylated JAK2 protein expression, while JAK2 protein expression did not show a significant change (Fig. 4C). The above results indicate that inhibiting the JAK2 signaling pathway can activate the activity of ROMK channels in DCT2 tubular membranes in low potassium diets.

Ang II mediates JAK2 signaling pathway inhibition of ROMK channel activity in DCT2 tubular epithelial cells

To further investigate whether Ang II in a low potassium diet inhibits the activity of the ROMK channel in the DCT2

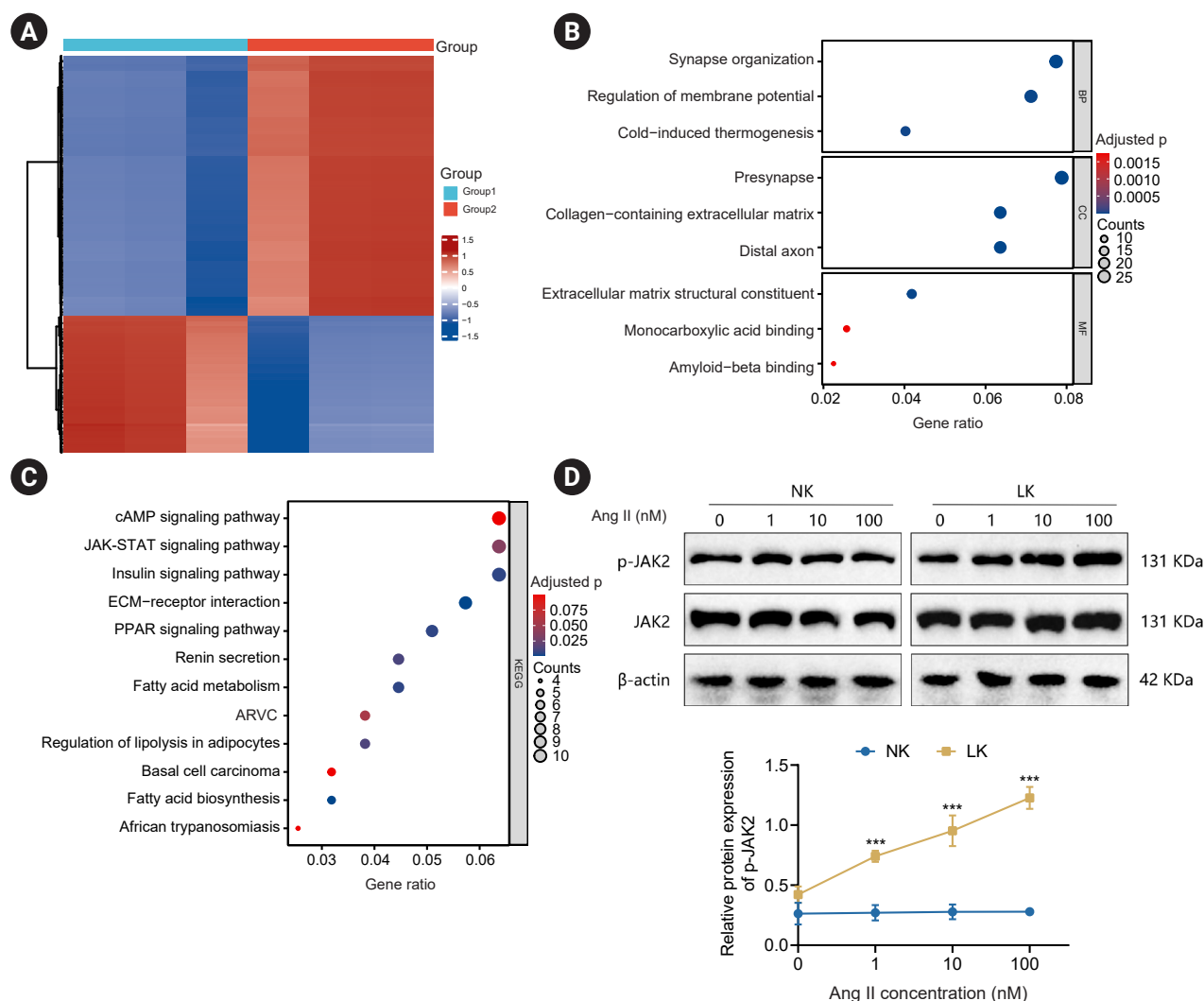


Figure 3. Identification of key pathways for Ang II-induced hypertension by transcriptome sequencing. (A) Heatmap of differentially expressed genes in the control group and the Ang II-treated group, with red indicating upregulation and blue indicating downregulation. Group 1 represents the control group, and group 2 represents the Ang II-treated group. (B) Gene Ontology enrichment analysis results of differentially expressed genes, with larger circles indicating more enrichment and bluer colors indicating more significant p-values. (C) Kyoto Encyclopedia of Genes and Genomes pathway enrichment analysis results of differentially expressed genes, with larger circles indicating more enrichment and bluer colors indicating more significant p-values. (D) Western blot analysis of p-JAK2 and JAK2 protein expression in the lumen membrane of distal convoluted tubule 2 in each group.

Ang II, angiotensin II; ARVC, arrhythmogenic right ventricular cardiomyopathy; cAMP, cyclic adenosine monophosphate; ECM, extracellular matrix; JAK2, janus kinase 2; LK, low potassium; NK, normal potassium; PPAR, peroxisome proliferator-activated receptor; STAT, signal transducer and activator of transcription.

***p < 0.001, significantly different between the two groups; n = 10.

tubular membrane through the JAK2 signaling pathway, we conducted experiments on DCT2 tubular membranes isolated from LK mice tissues. We treated them with both AG490 and Ang II. The experimental results showed that compared with the LK + control group, the ROMK channel

activity of the DCT2 tubular membrane and the whole-cell potassium current sensitive to TPNQ were significantly inhibited in the LK + Ang II group. However, compared with the LK + Ang II group, the DCT2 tubular membrane ROMK channel activity and TPNQ-sensitive whole-cell potassium

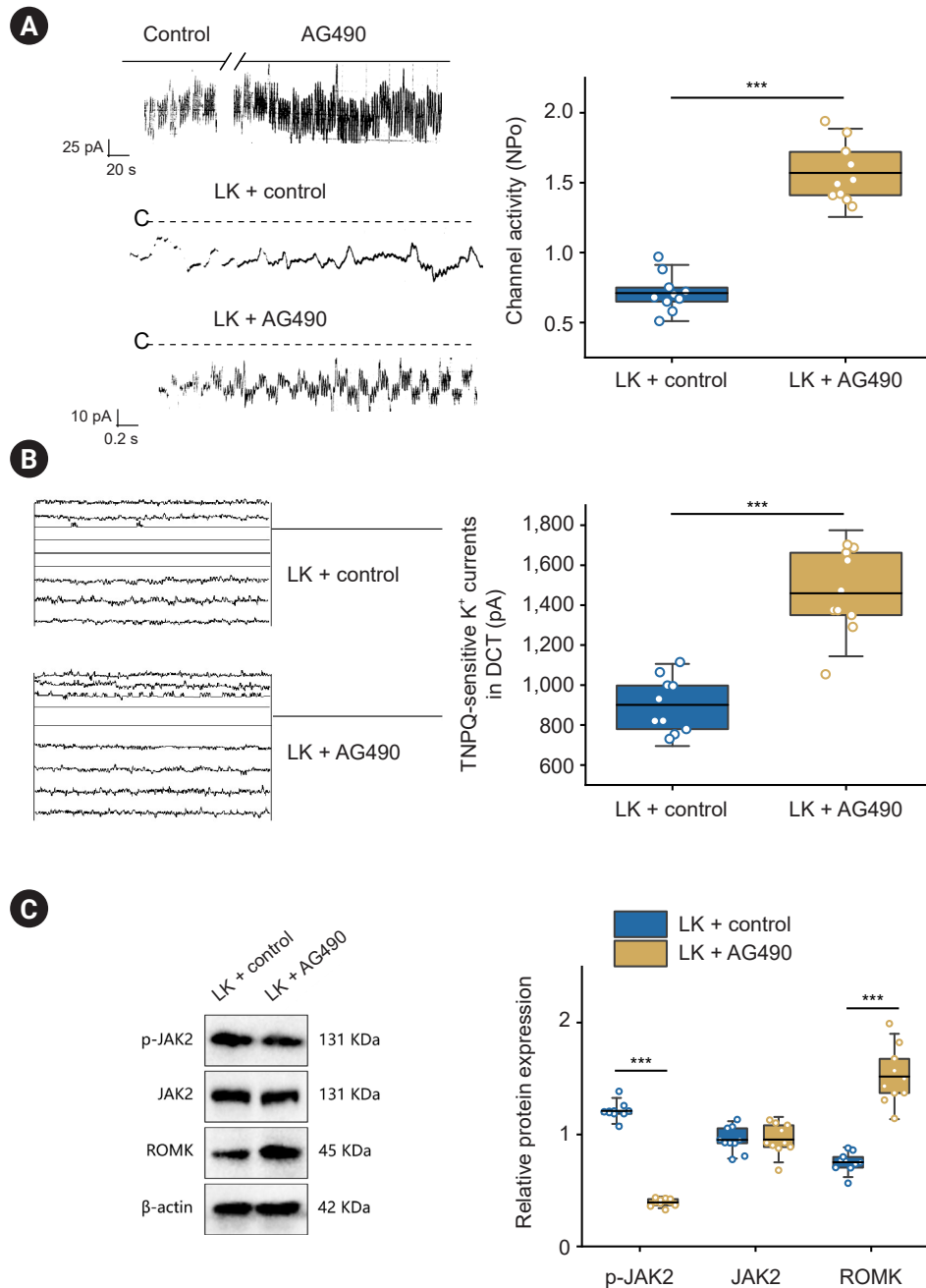


Figure 4. Suppression of ROMK channel activity in the lumen membrane of DCT2 by activation of JAK2 signaling pathway in a low potassium Diet. (A) Single-channel patch clamp technique was used to examine the effect of JAK2 inhibitor AG490 on ROMK channel activity in the lumen membrane of DCT2. indicate ROMK channel activity measured at different time points. The closed state of the channel ("C") is represented by a dashed line. The current ROMK channel activity is indicated by the short bar on the right side of each trace. (B) Measurement of the strength of tertiapin-Q (TPNQ)-sensitive K⁺ current in the lumen membrane of DCT2 treated with JAK2 inhibitor AG490, with the left panel showing the current changes and the right panel showing the statistical analysis. (C) Effect of JAK2 inhibitor AG490 on ROMK, p-JAK2, and JAK2 protein expression in the lumen membrane of DCT2 as detected by Western blotting. DCT, distal convoluted tubule; JAK2, janus kinase 2; LK, low potassium; NPo, number of channels × probability of openness; ROMK, renal outer medullary potassium channel.

***p < 0.001, significantly different between the two groups; n = 10.

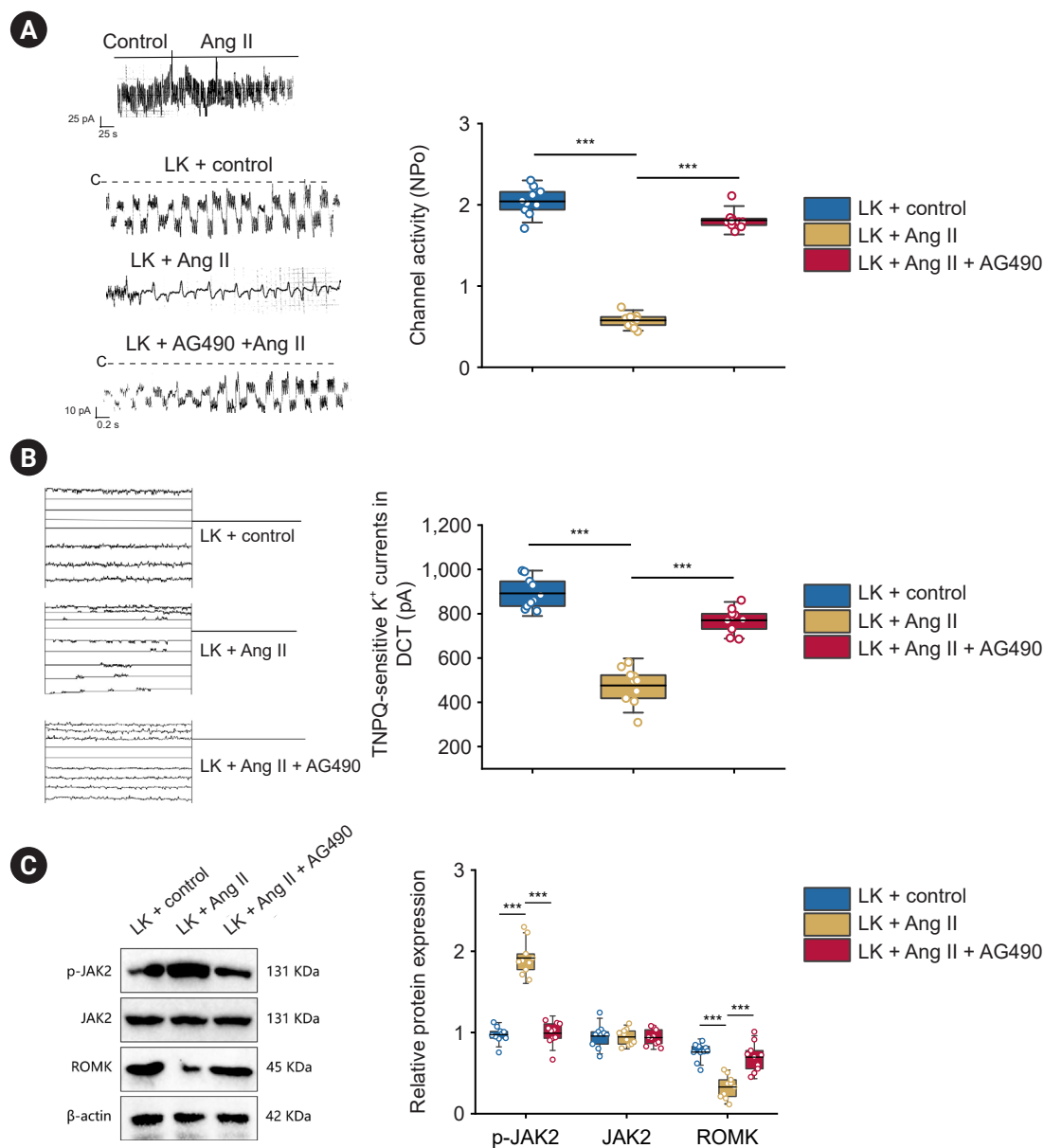


Figure 5. Ang II inhibits ROMK channel activity in the lumen of the DCT2 membrane by mediating the JAK2 signaling pathway in a low potassium diet. (A) The effect of AG490 and Ang II combined on ROMK channel activity in the lumen of the DCT2 membrane was detected using the patch clamp technique. The closed state of the channel ("C") is indicated by a dashed line. The current ROMK channel activity is represented by the short bar on the right side of each trace. (B) The effect of AG490 and Ang II combined on the intensity of tertiapin-Q (TPNQ)-sensitive K⁺ currents in the lumen of the DCT2 membrane was measured using the whole-cell patch clamp technique. The left graph shows the recording of current changes, and the right graph shows the statistical representation. (C) The effect of AG490 and Ang II combined on the expression of ROMK, p-JAK2, and JAK2 proteins in the lumen of the DCT2 membrane was detected using Western blot.

Ang II, angiotensin II; DCT, distal convoluted tubule; JAK2, janus kinase 2; LK, low potassium; NPo, number of channels × probability of openness; ROMK, renal outer medullary potassium channel.

***p < 0.001, significantly different between the two groups; n = 10.

currents in the LK + Ang II + AG490 group were significantly increased (Fig. 5A, B). In addition, Western blot analysis showed that compared with the LK + control group, the expression of ROMK protein in the DCT2 tubular membrane of the LK + Ang II group was significantly decreased, while the expression of p-JAK2 protein was significantly increased, but the expression of JAK2 protein remained unchanged. On the other hand, compared with the LK + Ang II group, the expression of ROMK protein in the DCT2 tubular membrane was significantly increased, while the expression of p-JAK2 protein was significantly decreased, and the expression of JAK2 protein remained unchanged in the LK + Ang II + AG490 group (Fig. 5C). These findings indicate that Ang II in a low potassium diet inhibits the activity of the DCT2 tubular membrane ROMK channel by mediating the JAK2 signaling pathway.

Ang II-mediated AT1R/JAK2 signaling pathway inhibits ROMK channel activity, affecting kidney K⁺ excretion

To test the relevance of the Ang II-mediated AT1R/JAK2 signaling pathway in the inhibition of ROMK channel activity *in vivo*, we treated LK-fed mice with an intraperitoneal injection of AG490 (10 mg/kg/day) for 8 days. We detected the protein expression of ROMK, AT1R, p-JAK2, and JAK2 in the renal cortex tissues of each group of mice using immunohistochemistry and Western blot. The results showed that compared with the LK group, the expression of ROMK protein in the DCT2 apical membrane was significantly decreased in the LK + Ang II group, while the protein expression of AT1R and p-JAK2 increased significantly, but there was no change in JAK2 protein expression. Compared with the LK + Ang II group, the expression of ROMK protein in the DCT2 apical membrane was significantly increased in the LK + Ang II + AG490 group, and there was no significant change in AT1R protein expression, while the protein expression of p-JAK2 decreased significantly, but there was no change in JAK2 protein expression (Fig. 6A, B). We also measured the ROMK channel activity and the TPNQ-sensitive potassium current intensity in the DCT2 apical membrane of each group of mice. The results showed that compared with the LK group, ROMK channel activity and TPNQ-sensitive potassium current intensity in the DCT2 tubular membrane of mice in the LK + Ang II group were significantly inhibited. Compared with the LK + Ang II group, the ROMK channel activity and TPNQ-sensitive po-

tassium current intensity in the DCT2 tubular membrane of mice in the LK + Ang II + AG490 group were significantly increased (Fig. 6C, D).

In addition, we also compared the urinary potassium excretion of each group of mice kidneys. The results showed that compared to the LK group, the urine potassium excretion in the kidney of mice in the LK + Ang II group was significantly reduced. Compared to the LK + Ang II group, the urine potassium excretion in the kidney of mice in the LK + Ang II + AG490 group was significantly increased (Fig. 6E).

Discussion

Our research has found that Ang II in low potassium diets can suppress the activity of the ROMK channel in the membrane of the DCT2 tubule. Previous studies have indicated that Ang II inhibits the activity of ROMK in the collecting duct by reducing the activation of cellular Src and suppresses K⁺ secretion mediated by ROMK [38]. In addition, the relationship between Ang II and the distal renal tubule has been reported. Ang II can affect the Na⁺ channel of the distal renal tubule through a mechanism that is not dependent on aldosterone [39]. Previous studies have not conducted relevant experiments, but past research has shown the significant impact of sodium ions on DCT2 besides potassium ions in the diet. The epithelial sodium channel restricts the rate of Na⁺ absorption in the aldosterone-sensitive distal nephron segments, including DCT2 [40]. Proper regulation of the epithelial sodium channel is crucial for fine-tuning renal sodium excretion, thereby maintaining sodium homeostasis within the body and long-term control of arterial blood pressure. Dietary Na⁺ enhances the tension of the apical P2Y2 receptor, inhibiting the opening probability of renal epithelial sodium channels and leading to elevated blood pressure.

In our *in vitro* cell experiments, we found that Ang II inhibits the DCT2 tubular membrane ROMK channel activity by activating AT1R receptors. This result indicates that Ang II is the positive regulator of AT1R, while AT1R is the negative regulator of ROMK channel activity. Consistent with other research findings, exogenous Ang II can activate AT1R receptors. Activation of the Ang II-AT1R signaling pathway can mediate disruption of the blood-brain barrier, neuroinflammation, and autonomic dysfunction in spontaneously hypertensive mice. In addition, there are also

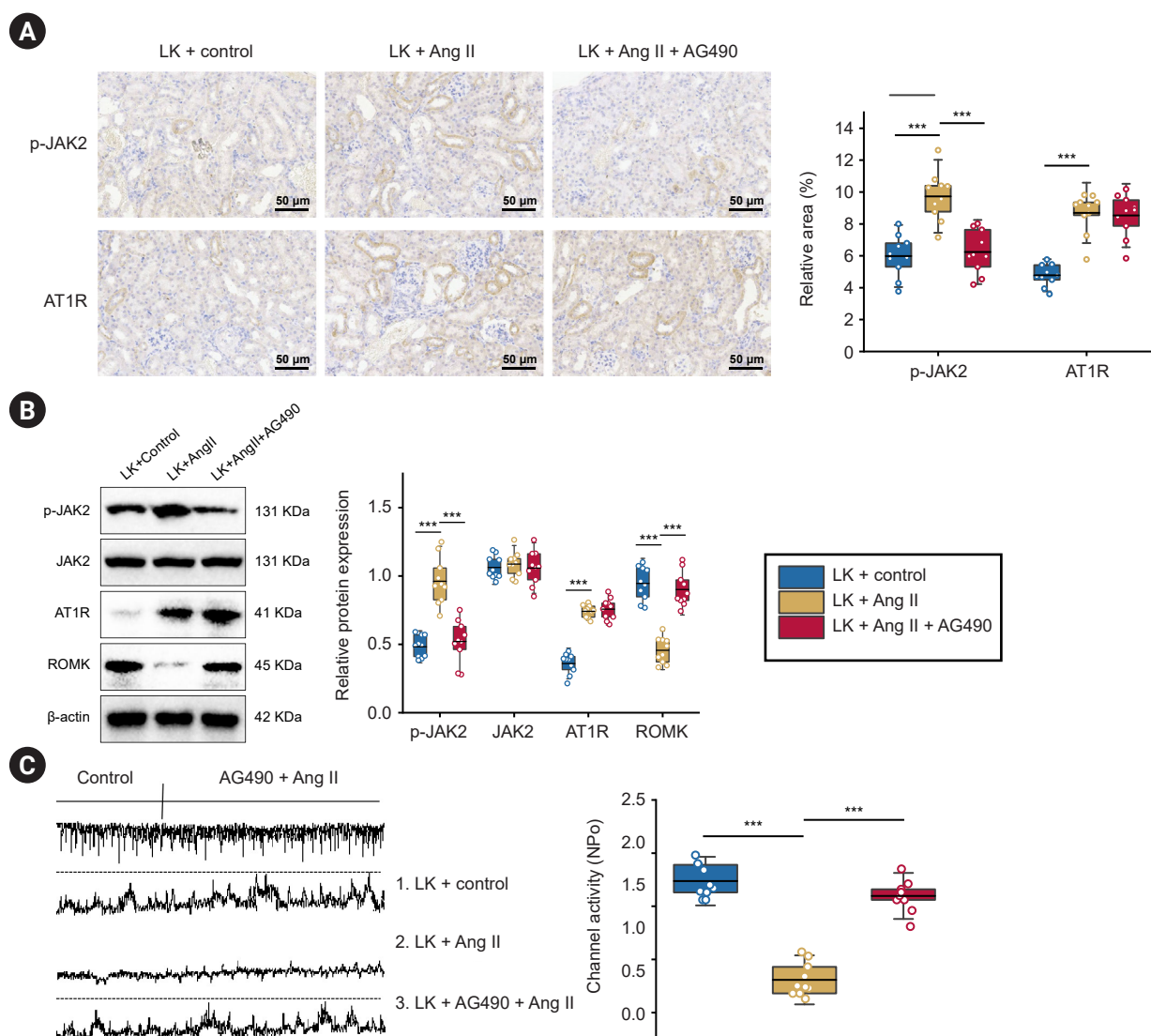


Figure 6. Ang II inhibits ROMK channel activity mediated by the AT1R/JAK2 signaling pathway. (A) The effect of AG490 and Ang II combined on the expression of AT1R and p-JAK2 proteins in mouse renal cortex tissue was detected using immunohistochemistry. (B) The effect of AG490 and Ang II combined on the expression of ROMK, AT1R, p-JAK2, and JAK2 proteins in mouse renal cortex tissue was detected using Western blot. (C) The effect of AG490 and Ang II combined on ROMK channel activity in the lumen of mouse distal convoluted tubule (DCT) 2 membrane was detected using the patch clamp technique. The ROMK channel activities detected at different time points are labeled as 1–3. The closed state of the channel (“C”) is indicated by a dashed line. The current ROMK channel activity is represented by the short bar on the right side of each trace. (D) The effect of AG490 and Ang II combined on the intensity of tertiapin-Q (TPNQ)-sensitive K⁺ currents in the lumen of mouse DCT2 membrane was measured using the whole-cell patch clamp technique. The left graph shows the recording of current changes, and the right graph shows the statistical representation. (E) The urinary potassium excretion in the different groups of mice was measured.

Ang II, angiotensin II; AT1R, Ang II type 1 receptor; BW, body weight; JAK2, janus kinase 2; LK, low potassium; NPo, number of channels × probability of openness; ROMK, renal outer medullary potassium channel.

***p < 0.001, significantly different between the two groups; n = 10.

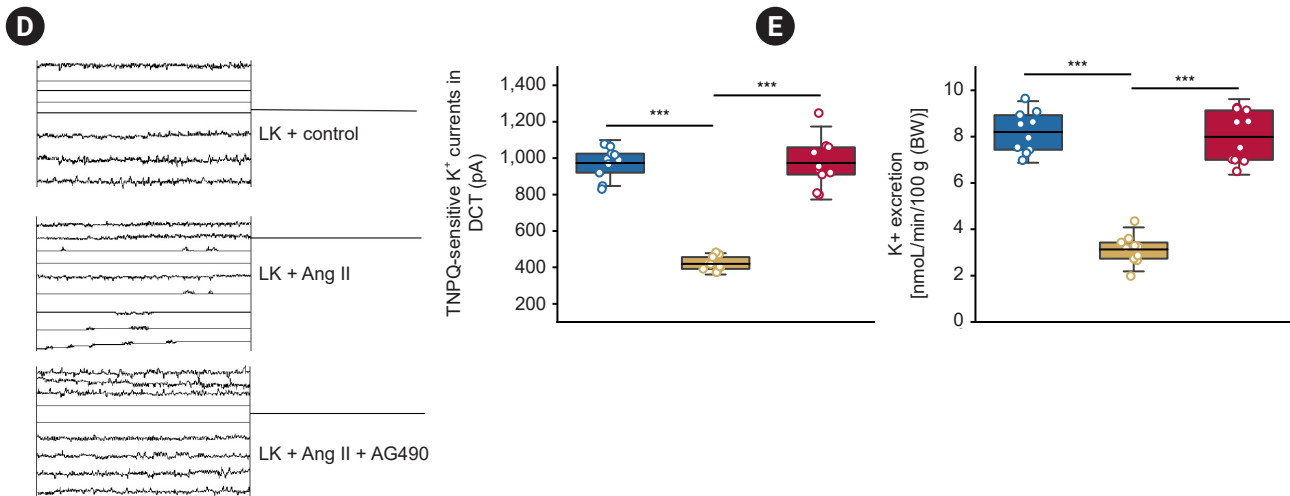


Figure 6. (Continued).

studies reporting that Ang II can inhibit ROMK and mediate K⁺ secretion [38].

Our bioinformatics analyses combined with results from *in vitro* cell experiments suggest that the JAK2 signaling pathway may be a critical pathway involved in Ang II-induced hypertension, and inhibition of the JAK2 signaling pathway can activate the activity of the ROMK channel in the DCT2 tubular membrane. This result indicates that Ang II is a positive regulator of JAK2, while JAK2 is a negative regulator of ROMK channel activity. Consistent with our research results, previous studies have reported the relationship between Ang II and JAK2. Ang II can activate the JAK2/STAT3 pathway, inducing the production of interleukin-6 in mice brainstem astrocytes. When Ang II expression is reduced, it can inhibit inflammation mediated by the JAK2 signaling pathway. More importantly, research has shown that the expression of JAK2 is involved in the development of Ang II-dependent hypertension.

In the kidney, Ang II inhibits channel activity through signaling cascades initiated by AT1R binding, including the activation of phospholipase C-protein kinase C, PTK, and NADPH oxidase. This inhibition hinders the phosphorylation of the ROMK channel, enhances its endocytosis, and reduces potassium secretion, leading to elevated blood pressure [20,35]. This study identifies Ang II, AT1R, and JAK2 as targets for hypertension treatment. Clinically, inhibiting the Ang II and AT1R-related pathways effectively improves hypertension, offering valuable insights for

hypertension therapy. In addition, *in vivo* and *in vitro* experiments further confirm that the Ang II-mediated AT1R/JAK2 signaling pathway inhibits ROMK channel activity, affecting renal K⁺ excretion. *In vitro* experiments found that vascular smooth muscle JAK2 reverses Ang II-induced hypertension by increasing reactive oxygen species levels. In addition, studies have found that the loss of vascular smooth muscle JAK2 can prevent Ang II-mediated neointimal hyperplasia in mice after injury. Moreover, in animal models, Ang II can induce TH17 activation and promote colonic inflammation via activating the JAK2/STAT pathway.

This study revealed the mechanism by which Ang II inhibits the activity of ROMK channels in the distal renal tubules during a low potassium diet through the AT1R-mediated JAK2 pathway, providing new insights and experimental evidence for a deeper understanding of the regulation of potassium ions in the kidney. It has important implications in elucidating the biological functions and pharmacological effects of Ang II. In addition, this study revealed the potential molecular mechanism of hypertension. The JAK2 signaling pathway is a key pathway induced by Ang II in the development of hypertension, and this discovery provides an important reference for screening drug targets for hypertension. However, there are limitations to this study, such as the fact that the conclusions are based on animal models and *in vitro* cell experiments, and further validation is needed for their reproducibility and

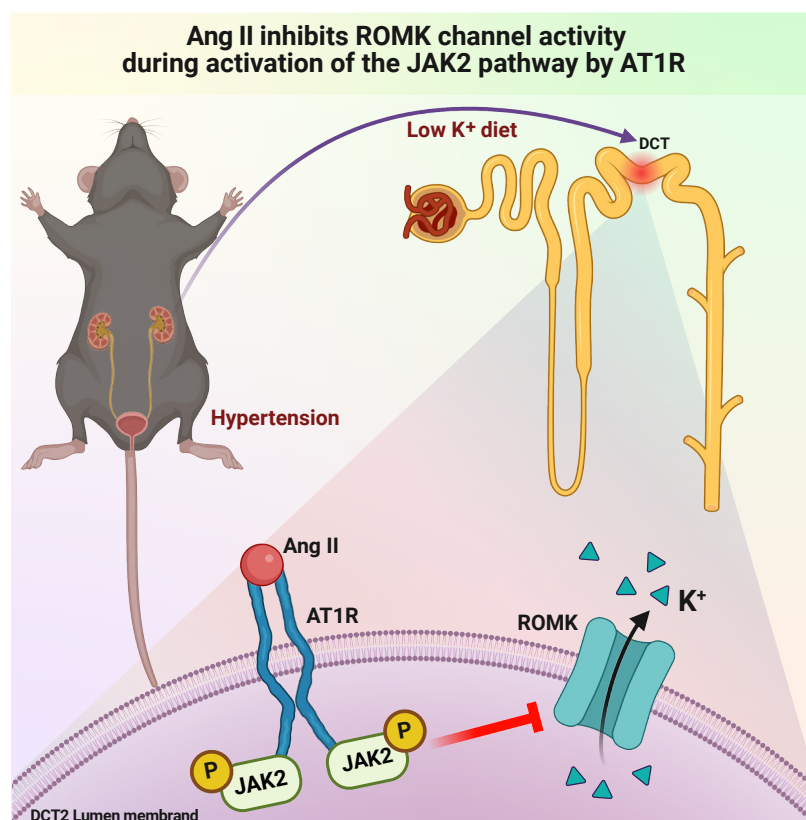


Figure 7. Molecular mechanism diagram showing that Ang II inhibits the activity of ROMK in the DCT during a low potassium diet via activation of the JAK2 pathway through AT1R.

Ang II, angiotensin II; AT1R, Ang II type 1 receptor; DCT, distal convoluted tubule; JAK2, janus kinase 2; ROMK, renal outer medullary potassium channel.

applicability in human experiments. In addition, this study did not address how to use relevant mechanisms to treat and prevent related diseases such as hypertension; further research is needed. In the future, based on this research, we can further explore the regulatory effects of other factors on the JAK2 signaling pathway and seek more effective methods for treating and preventing related diseases such as hypertension. Moreover, more profound research on transcriptomics and proteomics can also be conducted to investigate the regulation mechanism of potassium ions in the kidney from a global and dynamic perspective, providing a more comprehensive and systematic solution for the study and clinical treatment of kidney diseases.

Based on the above results, we can conclude that Ang II is a positive regulator of JAK2. Ang II promotes the activation of the JAK2 signaling pathway by binding with its receptor AT1R, which suppresses the activity of ROMK channels in

the renal DCT, inhibits K⁺ excretion, and may improve hypertension (Fig. 7). Our research findings underscore the physiological significance of Ang II in maintaining renal Na⁺ and K⁺ homeostasis. In future studies, the site-specific regulation of ion channels such as Na⁺ and K⁺ in different locations within the kidney and vasculature, along with their potential mechanisms and impact on hypertension, warrant further investigation.

Conflicts of interest

All authors have no conflicts of interest to declare.

Funding

This study was funded by the Doctoral Foundation of Qiqihar Academy of Medical Sciences (No. QMSI2023E-02),

Qiqihar Municipal Science and Technology Bureau joint guidance project (No. LSF GG-2023041), Key Cultivation Foundation of Qiqihar Academy of Medical Sciences (No. 2024-ZDPY-002), Doctoral Foundation of Qiqihar Academy of Medical Sciences (No. QMSI2022B-03), and the Heilongjiang Provincial Natural Science Foundation of China (No. LH2021H120).

Data sharing statement

The data presented in this study are available from the corresponding author upon reasonable request.

Authors' contributions

Conceptualization, Methodology: KZ

Data curation: LJ

Formal analysis: LW

Funding acquisition: XL

Investigation: TH

Visualization: RG

Writing-original draft: XL

Writing-review & editing: KZ, XL

All authors read and approved the final manuscript.

ORCID

Kun Zhao, <https://orcid.org/0009-0007-9662-3032>

Tiantian Han, <https://orcid.org/0000-0001-9622-2457>

Linzhen Jia, <https://orcid.org/0009-0001-3053-5773>

Libo Wen, <https://orcid.org/0009-0004-3392-3677>

Renjun Gao, <https://orcid.org/0000-0002-9029-9338>

Xue Li, <https://orcid.org/0009-0002-0710-1907>

References

1. GBD 2017 Diet Collaborators. Health effects of dietary risks in 195 countries, 1990-2017: a systematic analysis for the Global Burden of Disease Study 2017. *Lancet* 2019;393:1958-1972.
2. Guo QH, Zhang YQ, Wang JG. Asian management of hypertension: current status, home blood pressure, and specific concerns in China. *J Clin Hypertens (Greenwich)* 2020;22:475-478.
3. Wang Z, Chen Z, Zhang L, et al. Status of hypertension in China: results from the China hypertension survey, 2012-2015. *Circulation* 2018;137:2344-2356.
4. Zheng E, Xu J, Xu J, et al. Health-related quality of life and its influencing factors for elderly patients with hypertension: evidence from Heilongjiang Province, China. *Front Public Health* 2021;9:654822.
5. Poulter NR, Prabhakaran D, Caulfield M. Hypertension. *Lancet* 2015;386:801-812.
6. Al Ghorani H, Götzinger F, Böhm M, Mahfoud F. Arterial hypertension: clinical trials update 2021. *Nutr Metab Cardiovasc Dis* 2022;32:21-31.
7. Welling PA. Roles and regulation of renal K channels. *Annu Rev Physiol* 2016;78:415-435.
8. Nüsing RM, Pantalone F, Gröne HJ, Seyberth HW, Wegmann M. Expression of the potassium channel ROMK in adult and fetal human kidney. *Histochem Cell Biol* 2005;123:553-559.
9. O'Donnell BM, Mackie TD, Subramanya AR, Brodsky JL. Endoplasmic reticulum-associated degradation of the renal potassium channel, ROMK, leads to type II Bartter syndrome. *J Biol Chem* 2017;292:12813-12827.
10. Wu P, Gao ZX, Su XT, et al. Role of WNK4 and kidney-specific WNK1 in mediating the effect of high dietary K+ intake on ROMK channel in the distal convoluted tubule. *Am J Physiol Renal Physiol* 2018;315:F223-F230.
11. Lu M, Wang T, Yan Q, et al. Absence of small conductance K+ channel (SK) activity in apical membranes of thick ascending limb and cortical collecting duct in ROMK (Bartter's) knockout mice. *J Biol Chem* 2002;277:37881-37887.
12. Kaufman MB. Pharmaceutical approval update. *P T* 2018;43:528-530.
13. Yugandhar VG, Clark MA. Angiotensin III: a physiological relevant peptide of the renin angiotensin system. *Peptides* 2013;46:26-32.
14. Shanks J, Ramchandra R. Angiotensin II and the cardiac parasympathetic nervous system in hypertension. *Int J Mol Sci* 2021;22:12305.
15. Eckenstaler R, Sandori J, Gekle M, Benndorf RA. Angiotensin II receptor type 1: an update on structure, expression and pathology. *Biochem Pharmacol* 2021;192:114673.
16. Zhang L, Wang Y, Wu G, et al. Blockade of JAK2 protects mice against hypoxia-induced pulmonary arterial hypertension by repressing pulmonary arterial smooth muscle cell proliferation. *Cell Prolif* 2020;53:e12742.
17. Milara J, Ballester B, Morell A, et al. JAK2 mediates lung fibrosis, pulmonary vascular remodelling and hypertension in idiopathic pulmonary fibrosis: an experimental study. *Thorax* 2018;73:519-529.

18. Momose R, Inami T, Takeuchi K, et al. Combination therapy with pulmonary vasodilatation and JAK2 inhibition for pulmonary hypertension with polycythemia vera. *CJC Open* 2022;5:90-92.
19. Wang W, Lu Y, Hu X, et al. Interleukin-22 exacerbates angiotensin II-induced hypertensive renal injury. *Int Immunopharmacol* 2022;109:108840.
20. Wei Y, Zvilowitz B, Satlin LM, Wang WH. Angiotensin II inhibits the ROMK-like small conductance K channel in renal cortical collecting duct during dietary potassium restriction. *J Biol Chem* 2007;282:6455-6462.
21. Zhang SL, Guo J, Moini B, Ingelfinger JR. Angiotensin II stimulates Pax-2 in rat kidney proximal tubular cells: impact on proliferation and apoptosis. *Kidney Int* 2004;66:2181-2192.
22. Zhang DD, Zheng JY, Duan XP, Lin DH, Wang WH. ROMK channels are inhibited in the aldosterone-sensitive distal nephron of renal tubule Nedd4-2-deficient mice. *Am J Physiol Renal Physiol* 2022;322:F55-F67.
23. Luo LL, Zhao L, Wang YX, et al. Insulin-like growth factor binding protein-3 is a new predictor of radiosensitivity on esophageal squamous cell carcinoma. *Sci Rep* 2015;5:17336.
24. Su H, Jin X, Zhang X, et al. FH535 increases the radiosensitivity and reverses epithelial-to-mesenchymal transition of radio-resistant esophageal cancer cell line KYSE-150R. *J Transl Med* 2015;13:104.
25. Murthy M, Kurz T, O'Shaughnessy KM. ROMK expression remains unaltered in a mouse model of familial hyperkalemic hypertension caused by the CUL3Δ403-459 mutation. *Physiol Rep* 2016;4:e12850.
26. van der Wijst J, Tutakhel OA, Bos C, et al. Effects of a high-sodium/low-potassium diet on renal calcium, magnesium, and phosphate handling. *Am J Physiol Renal Physiol* 2018;315:F110-F122.
27. Akaike N, Hirata A, Kiyohara T, Oyama Y. Neural regulation on the active sodium-potassium transport in hypokalaemic rat skeletal muscles. *J Physiol* 1983;341:245-255.
28. Hong M, Tao S, Zhang L, et al. RNA sequencing: new technologies and applications in cancer research. *J Hematol Oncol* 2020;13:166.
29. Pareek CS, Smoczynski R, Tretyn A. Sequencing technologies and genome sequencing. *J Appl Genet* 2011;52:413-435.
30. Tan L, Xu Q, Wang Q, Shi R, Zhang G. Identification of key genes and pathways affected in epicardial adipose tissue from patients with coronary artery disease by integrated bioinformatics analysis. *PeerJ* 2020;8:e8763.
31. Dai F, Wu J, Deng Z, et al. Integrated bioinformatic analysis of DNA methylation and immune infiltration in endometrial cancer. *Biomed Res Int* 2022;2022:5119411.
32. Wang J, Polaki V, Chen S, Bihl JC. Exercise improves endothelial function associated with alleviated inflammation and oxidative stress of perivascular adipose tissue in type 2 diabetic mice. *Oxid Med Cell Longev* 2020;2020:8830537.
33. Shao JB, Li Z, Zhang N, Yang F, Gao W, Sun ZG. Hypoxia-inducible factor 1α in combination with vascular endothelial growth factor could predict the prognosis of postoperative patients with oesophageal squamous cell cancer. *Pol J Pathol* 2019;70:84-90.
34. Yin H, Ma J, Chen L, et al. MiR-99a enhances the radiation sensitivity of non-small cell lung cancer by targeting mTOR. *Cell Physiol Biochem* 2018;46:471-481.
35. Wei Y, Bloom P, Lin D, Gu R, Wang WH. Effect of dietary K intake on apical small-conductance K channel in CCD: role of protein tyrosine kinase. *Am J Physiol Renal Physiol* 2001;281:F206-F212.
36. Wei X, Jin J, Wu J, et al. Cardiac-specific BACH1 ablation attenuates pathological cardiac hypertrophy by inhibiting the Ang II type 1 receptor expression and the Ca²⁺/CaMKII pathway. *Cardiovasc Res* 2023;119:1842-1855.
37. Cantero-Navarro E, Fernández-Fernández B, Ramos AM, et al. Renin-angiotensin system and inflammation update. *Mol Cell Endocrinol* 2021;529:111254.
38. Polidoro JZ, Rebouças NA, Girardi AC. The angiotensin II type 1 receptor-associated protein attenuates angiotensin II-mediated inhibition of the renal outer medullary potassium channel in collecting duct cells. *Front Physiol* 2021;12:642409.
39. Wu P, Gao ZX, Zhang DD, et al. Effect of angiotensin II on ENaC in the distal convoluted tubule and in the cortical collecting duct of mineralocorticoid receptor deficient mice. *J Am Heart Assoc* 2020;9:e014996.
40. Nesterov V, Krueger B, Bertog M, Dahlmann A, Palmisano R, Korbmacher C. In liddle syndrome, epithelial sodium channel is hyperactive mainly in the early part of the aldosterone-sensitive distal nephron. *Hypertension* 2016;67:1256-1262.